

San Francisco Bay Area Earthquake Simulations: A step toward a Standard Physical Earthquake Model

Steven N. Ward

Institute of Geophysics and Planetary Physics, University of California, Santa Cruz, CA, USA
(email: ward@uplift.ucsc.edu, phone: 831-459-2480, fax: 831-459-3074).

Abstract

Earthquakes in California's San Francisco Bay Area are likely to be more strongly affected by elastic stress interaction than earthquakes in any other place in the world because of the region's closely spaced, sub-parallel distribution of faults. I believe therefore, that meaningful quantification of earthquake probability and hazard in the Bay Area can be made only with the guidance provided by physically-based and region-wide earthquake models that account for this interaction. This paper represents a first step in developing a *Standard Physical Earthquake Model* for the San Francisco Bay Area through realistic, 3000-year simulations of earthquakes on all of the area's major faults.

Introduction

Due to the region's closely spaced, sub-parallel distribution of faults (Figure 1), earthquakes of the San Francisco Bay are likely to be more strongly affected by fault stress interaction than earthquakes in any other place in the world. Given this, I believe that meaningful progress toward updating earthquake probabilities in the Bay Area can be made only with the guidance provided by physically-based and region-wide earthquake simulations. As a first step toward realizing a *Standard Physical Earthquake Model* for the San Francisco Bay Area, this paper offers a set of seismicity simulations. These simulations demonstrate that a *Standard Physical Earthquake Model* is entirely feasible, they illustrate its application, and they blueprint its construction.

2 Theoretical Foundation

Earthquakes interact in the sense that stresses shed from a fault during one event either advance or delay the occurrence of nearby earthquakes. Many researchers have applied this concept to fault systems by mapping areas of stress enhancement or stress shadow caused by historical earthquakes. Stress interaction is a major component of a *Standard Physical Earthquake Model* and so it builds directly on these works. In fact, the theoretical and computational aspects of stress interaction employed here offer no significant advancement. This paper does however, include three primary extensions to previous efforts:

- The timing and slip distribution of earthquakes are not specified by the user, but rather earthquakes occur spontaneously. Fault strength, fault friction law, and the existing state of stress solely determine the timing and extent of earthquake ruptures.
- Stress states are considered not only before and after earthquakes, but within each earthquake as well. This model generates detailed rupture histories from nucleation to healing.
- Applied interseismic stresses are not uniform. Instead, variable tectonic stresses drive each fault in the system at a velocity compatible with its estimated geological slip rate.

At their most basic level, all seismicity simulations involve a balance between fault driving stresses and fault frictional strength. For a fault system with many fault elements, the force balance equations take a vector form

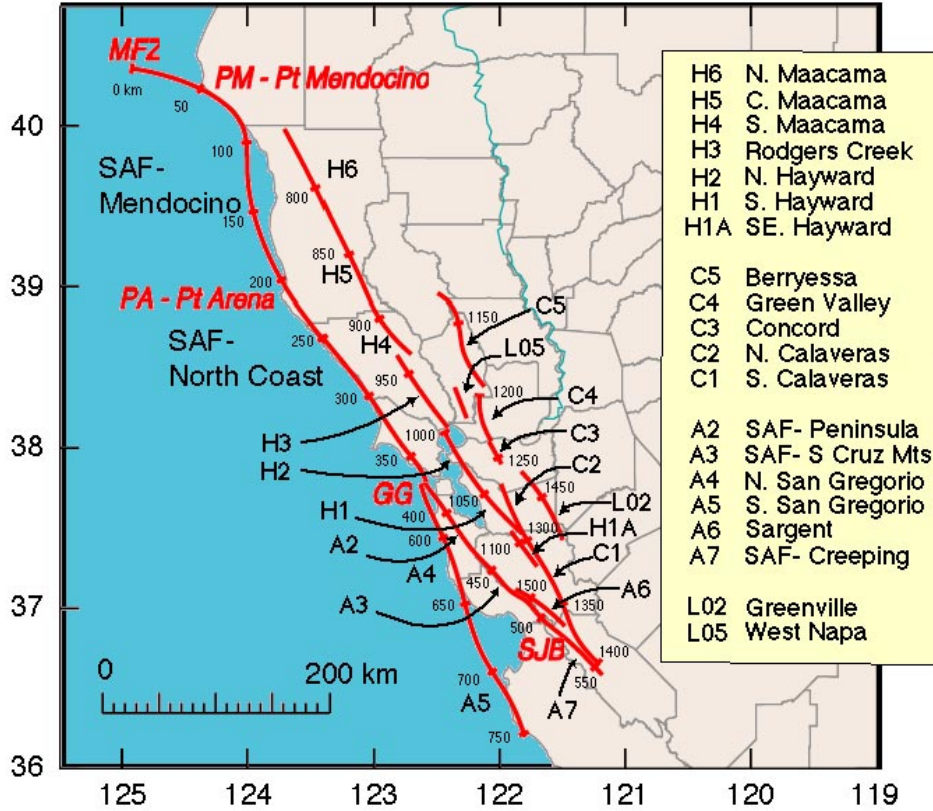


Figure 1. Base map showing the faults included in the San Francisco Bay Area earthquake simulations. Fault codes H6, A2, etc., come from the 1996 report of the Working Group on Northern California Earthquake Potential. Small numbers label distance in km. This fault system includes a 3km right step in the San Andreas Fault at the Golden Gate (km #375).

$$\mathbf{T}(t) = \mathbf{T}_0 + \mathbf{R} [\mathbf{u}(t) - t\mathbf{v}_{\text{plate}}] = \mathbf{Q}(\mathbf{S}_s, \mathbf{S}_d, \mathbf{u}(t), \mathbf{v}(t), \mathbf{T}(t)) \quad (1)$$

In (1): \mathbf{T}_0 is the Coulomb stress at \mathbf{x}_i at the start of the simulation; $\mathbf{R} = \mathbf{R}_{ij}(\mathbf{x}_i, \mathbf{x}_j)$ is the travel time delayed Coulomb stress induced at \mathbf{x}_i from a unit positive slip on the j -th fault element; $\mathbf{v}_{\text{plate}}$ is the geological slip rate of the fault elements; $\mathbf{u}(t)$ is total displacement since the start of the simulation; and $\mathbf{v}(t)$ is the current slip velocity. The \mathbf{S}_s and \mathbf{S}_d are the fixed static and dynamic strengths of the fault. They can however, vary along strike. Fault frictional strength \mathbf{Q} has many forms and it may include other state parameters beyond those listed. In any case, if $\mathbf{u}(t)$ increasingly lags $t\mathbf{v}_{\text{plate}}$, driving stress $\mathbf{T}(t)$ becomes increasingly large and positive until on some fault elements

$$T_i(t) > Q_i(\mathbf{S}_s, \mathbf{S}_d, \mathbf{u}(t), \mathbf{v}(t), \mathbf{T}(t)) \quad (2)$$

When condition (2) happens, $\mathbf{u}(t)$ advances to $\mathbf{u}(t+dt)$ to rebalance (1) -- i.e. an earthquake strikes. Depending upon the specifics of \mathbf{Q} , various numerical recipes might advance $\mathbf{u}(t)$. For this work, I use an iterative scheme developed under a modified quasi-static assumption to rebalance (1). For \mathbf{Q} , I adopt a two-parameter velocity weakening law.

The simulations here resemble those that I developed originally for use in southern California, however the newer models incorporate several improvements in the theoretical formulation including:

- 1) Allowance for a finite speed of signal propagation (v_p) while keeping within a quasi-static framework.
- 2) Association of a specific intra-seismic interval (dt) with each step in the rupture simulation.

- 3) Incorporation of fully localized fault friction.
- 4) Formation of explicit relationships among critical slip velocity, critical slip distance, and critical patch size for run-away failure in terms of v_p , dt and the difference between static and dynamic fault strengths.

3 Products

1906 San Francisco Earthquake

Physical models of earthquakes have the powerful ability to incorporate a wide range of information. One excellent source of information are samples of coseismic surface slip. Previous studies have demonstrated that when properly modeled, even a single observation of surface slip can go a long way toward constraining a fault's effective strength distribution. In this field region, the 1906 San Francisco earthquake serves as a guide.

Figure 2 details a simulation of the 1906 San Francisco earthquake over a 550 km long stretch of the San Andreas Fault from the Mendocino Fracture Zone to San Juan Bautista. (Similar detail exists for every earthquake in the 3000 year run.) The green color represents the current effective strength of the fault, i.e. $Q(t) - S_d$. Current effective strength equals $\Delta S = S_s - S_d$, a fixed physical characteristic except at points where the fault is slipping. The yellow color represents the current effective stress on the fault, i.e. $T(t) - S_d$. Current effective stress is not a fixed physical characteristic, it changes between, and within ruptures. In this case, I selected the initial distribution of effective stress (light gray, top line) and effective strength ΔS so that the model quake reproduced the surface slip of the 1906 San Francisco earthquake (squares, bottom). A good fit to the surface slip was possible with a single variation in effective strength, from 20 to 30 bars in northern Mendocino (km #90). Note that the Fort Ross slip deficit near km #250, can be generated by an initial stress selection alone, without resort to permanent, along-strike changes in effective strength. Matching the deficit however, did require that that section of the fault be empty of initial effective stress. The 3000 year simulations rarely report large sections of faults being completely empty or full of stress. For this reason, 20 to 30 bars represents minimum values for ΔS near Fort Ross, or indeed, for most of the fault north of the Golden Gate (GG).

As did the actual 1906 earthquake, the model earthquake nucleates near the Golden Gate and propagates bi-laterally toward the north and south. Note that the rupture speeds up where the stress barrier [$S_s - T(t)$] forward of the rupture is low, and slows down where the forward stress barrier is high. The "finger print" at the bottom of Figure 2 plots the evolution of slip at 2-second intervals. You can see that the rupture takes over a dozen seconds to breach the stress barrier at Fort Ross. Rupture actually jumped across the barrier near km#220 before the middle of the barrier finally collapsed. Admittedly, no one knows the slip history of the 1906 earthquake to this level of detail. Still, Figure 2 testifies that realistic rupture simulations are achievable within a modified quasi-static framework and that such simulations furnish physically defensible implications of other information (such as the Fort Ross slip deficit) on rupture evolution.

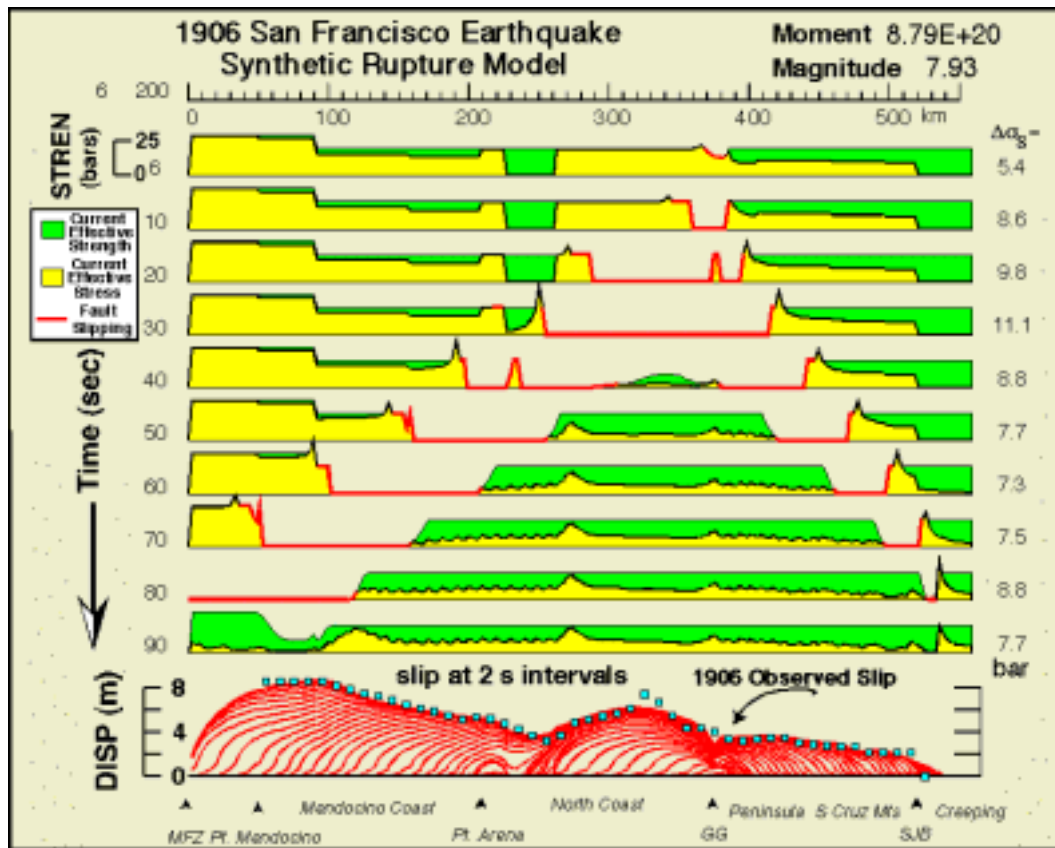


Figure 2. Simulation of the 1906 San Francisco earthquake over a 550 km long stretch of the San Andreas Fault from the Mendocino Fracture Zone (MFZ, left) to San Juan Bautista (SJB, right). The yellow color represents the current effective strength of the fault. The green color represents the current effective stress on the fault. The initial distribution of effective stress (light gray, top line) was selected so that the synthetic quake reproduced the surface slip of the 1906 San Francisco earthquake (squares, bottom) as inferred by geodetic analysis. Time since nucleation is listed to the left, and the red coloring highlights actively sliding parts of the fault.

3000 year simulation

Roughly ten samples of every type of fault rupture are needed to quantify earthquake recurrence statistics adequately. Certain earthquakes in the San Francisco Bay Area may have repeat times of several hundred years, so the task of earthquake probability estimation calls for catalogs spanning several thousand years. In the absence of a real catalog of this duration, the call goes out to physical earthquake models. Figure 3 replays a 3000 year sequence of earthquakes on the major faults of the San Francisco Bay Area starting with the system state remaining at the end of the 1906 rupture (bottom Figure 2). The “movie” frames do not space regularly in time, rather years or more than 150 years. It is not hard to visualize certain premonitions or cause and effects; say, the M7 San Andreas event in 334.5 announcing the impending arrival of a M7.7 in 338, or the M7.7 rupture in 730 “finishing its business” in 740.5 (M7.0) by breaking the Santa Cruz Mountains segment of the fault that it had missed earlier. Other patterns, such as large San Andreas quakes shutting off subsequent activity on the East Bay faults, are more subtle, but they make perfect fodder for pattern recognition schemes.

Figure 4 magnifies the final slip distribution of all $M > 6.5$ quakes on the San Andreas Fault. In close-up, the character of individual ruptures is far more expressive than the line plots of Figure 3 might suggest. Physical earthquake models provide a means to interpret these expressions. For example, previous experiments have shown that locations where the slip function is concave up tend to be left at a higher state of effective stress after the earthquake than they were prior to it. Concave-up locations attract subsequent “fill-in” earthquakes as exemplified by the event pairs in years 338 and 432, and 912 and 941. Being geometrically correct, rupture encyclopedias computed from physical

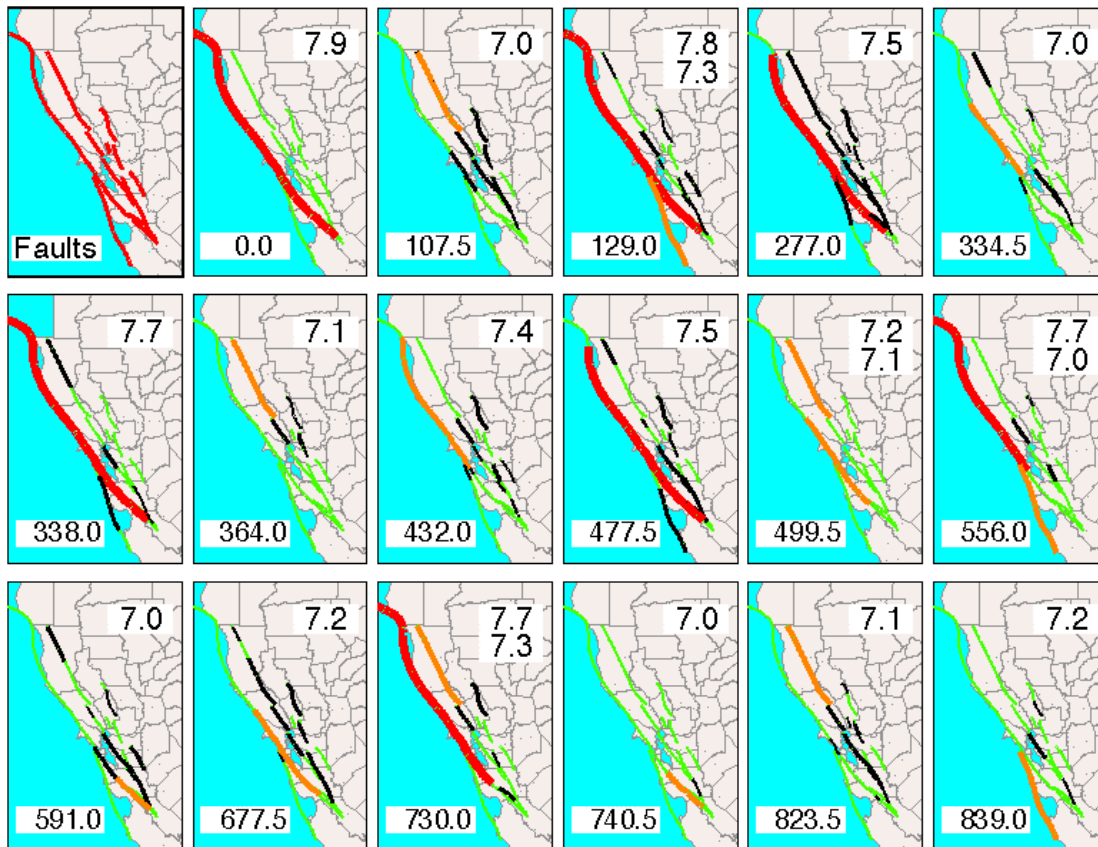


Figure 3. 3000 year sequence of earthquakes on the major faults of the San Francisco Bay Area following the 1906 event. The included faults appear in red in the upper left panel. The “movie” frames are not regularly spaced in time, but they update on the occurrence of an $M > 7$ event listed to the upper right in each frame. Red coloring marks $M > 7.5$ earthquakes; orange coloring, $7 < M < 7.5$; and the thick and thin black lines, $6.5 < M < 7$ and $6 < M < 6.5$ respectively. At the lower left in each panel is time in years since the start of the simulation. The interseismic time step interval is $\Delta T = 0.5$ yr.

earthquake models can be compared directly with site-specific paleoseismic studies that quantify slip-per-event and variation in slip-per-event.

4 Conclusions

Physical models represent the best existing means to quantify earthquake recurrence in a region characterized by closely spaced, sub-parallel faults. A *Standard Physical Earthquake Model* provides the mechanism to integrate fully the diverse disciplines within the earthquake research community. As a platform for data utilization and verification, a physical earthquake model can employ directly any earthquake property that is measurable in the field or in the laboratory to tune and test its seismicity

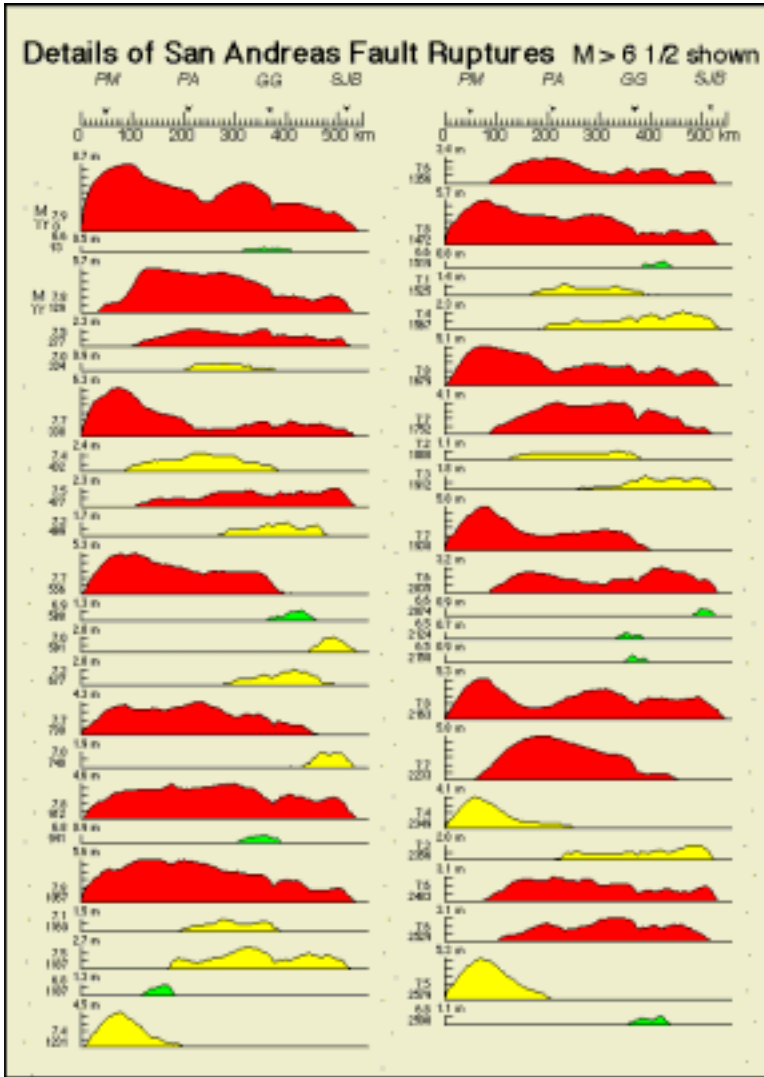


Figure 4. Details of the final slip distributions of all $M > 6.5$ quakes on the San Andreas Fault for the first 2600 years of the 3000 year simulation. Magnitude and year of occurrence are listed to the left of each trace. Red, yellow and green events are $M > 7.5$, $7 < M < 7.5$ and $6.5 < M < 7$ respectively. Rupture encyclopedias like this can be compared directly with site-specific paleoseismic studies that quantify slip-per-event and variation in slip-per-event.

products. As a platform for probability forecasts, a physical earthquake model can supply rational estimates of every imaginable earthquake statistic while simultaneously satisfying all slip and earthquake rate constraints. As a platform for hazard analysis, a physical earthquake model can compute earthquake shaking intensity from first principles by convolving a full suite of rupture scenarios with site-specific dislocation Green's functions. Probabilistic estimates of shaking intensity can be constructed directly from this set of synthetic seismograms without need for empirical attenuation relations.

Physical earthquake models have advanced greatly in the last decade. Simulations of earthquake generation and recurrence are now sufficiently credible that such calculations can begin to take substantial roles in scientific studies of earthquake probability and hazard. On the horizon lay vastly improved earthquake simulations that will lift the restrictive assumptions of this vanguard and carry the promise to full potential.